

# Phonon resonances in atomic currents through Bose-Fermi mixtures in optical lattices

M. Bruderer,<sup>1</sup> T. H. Johnson,<sup>2</sup> S. R. Clark,<sup>2,3</sup> D. Jaksch,<sup>2,3</sup> A. Posazhennikova,<sup>1</sup> and W. Belzig<sup>1</sup>

<sup>1</sup>Fachbereich Physik, Universität Konstanz, D-78457 Konstanz, Germany

<sup>2</sup>Clarendon Laboratory, University of Oxford, Parks Road, Oxford OX1 3PU, United Kingdom

<sup>3</sup>Centre for Quantum Technologies, National University of Singapore, 3 Science Drive 2, Singapore 117543

(Received 22 July 2010; published 21 October 2010)

We present an analysis of Bose-Fermi mixtures in optical lattices for the case where the lattice potential of the fermions is tilted and the bosons (in the superfluid phase) are described by Bogoliubov phonons. It is shown that the Bogoliubov phonons enable hopping transitions between fermionic Wannier-Stark states; these transitions are accompanied by energy dissipation into the superfluid and result in a net atomic current along the lattice. We derive a general expression for the drift velocity of the fermions and find that the dependence of the atomic current on the lattice tilt exhibits negative differential conductance and phonon resonances. Numerical simulations of the full dynamics of the system based on the time-evolving block decimation algorithm reveal that the phonon resonances should be observable under the conditions of a realistic measuring procedure.

DOI: 10.1103/PhysRevA.82.043617

PACS number(s): 67.85.Pq, 05.60.Gg, 72.10.-d

## I. INTRODUCTION

One of the most intriguing prospects opened up by recent advances in atomic physics is the possibility of studying many-body quantum systems. In particular, ultracold atoms confined to optical lattice potentials have been shown to be perfectly suitable for implementing physical models of fundamental interest not only to the field of atomic physics but also to condensed matter physics [1,2]. Specific examples of a highly versatile many-body system include Bose-Fermi mixtures in optical lattices, which have been used recently to analyze the effect of fermionic impurities on the superfluid to Mott-insulator transition [3–5]. A further experimental setup closely related to condensed matter systems consists of ultracold atoms in *tilted* optical lattice potentials. Several fundamental quantum mechanical processes related to nonequilibrium transport of particles have been observed in this setup such as, e.g., Landau-Zener tunneling [6], Bloch oscillations [7,8], and processes analogous to photon-assisted tunneling [9].

Of particular importance, collisionally induced transport of fermions confined to an optical lattice and coupled to an ultracold bosonic bath has been observed in an experimental setup of a similar type to the one considered in this article [10]. Furthermore, a closely related theoretical analysis of collision-induced atomic currents along a tilted optical lattice was provided by Ponomarev *et al.* [11] based on a random matrix approach. In essence it was pointed out in Ref. [11] that the atomic current exhibits Ohmic and negative differential conductance (NDC).

In the present article we study a natural extension of the mentioned experiments, namely lattice Bose-Fermi mixtures with the fermions confined to a tilted optical potential. Motivated by earlier considerations [12,13] we show that this system is highly appropriate for exploring the effects of electron-phonon interactions on nonequilibrium electric transport through a conductor. Specifically, we demonstrate that electron-phonon resonances, predicted to exist in solids nearly 40 years ago [14–16], yet for which there seems to be no conclusive experimental evidence [17,18], can be realized using ultracold atoms.

In our model the fermions take the role of electrons, whereas the bosons provide a nearly perfect counterpart to acoustic phonons in solids. The tilt imposed on the lattice potential of the fermions corresponds to an applied bias voltage to the system. The collisions between fermions and bosons result in fermion-phonon relaxation processes, which give rise to a net atomic current along the tilted lattice potential [11,13,19], as illustrated in Fig. 1. We show that in our case, where both the fermions and bosons are trapped in an optical lattice, phonon resonances in the atomic current occur. They arise as the momentum of the phonon emitted in the relaxation process approaches a so-called Van Hove singularity [20] at the upper edge of the phonon band. Moreover, we shall see that phonon resonances, at least on the level of approximations made in this article, are also expected to occur in Bose-Bose mixtures [21].

There are crucial advantages of our cold atom implementation over a solid-state system: First, neither impurities nor imperfections in the system suppress the resonances in the current [17] and hence fermion-phonon scattering is the only relaxation process, which can be fully controlled via the bosonic system parameters [5,22]. Second, large lattice tilts

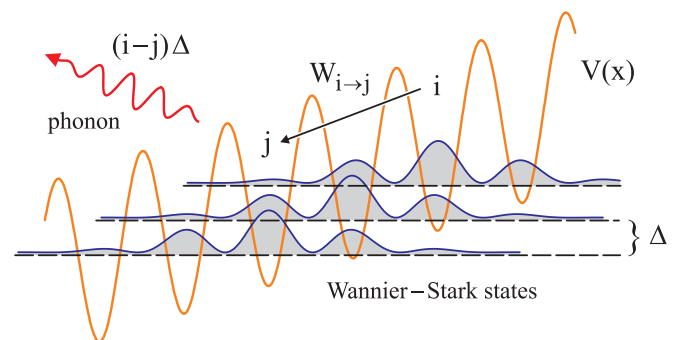


FIG. 1. (Color online) Fermions confined to a tilted potential  $V(x)$  form a Wannier-Stark ladder with a constant energy separation  $\Delta$  between adjacent lattice sites. The fermion-boson interaction enables phonon-assisted transitions from site  $i$  to  $j$  at the rate  $W_{i \rightarrow j}$ . The released energy  $(i-j)\Delta$  is dissipated in the form of a phonon emitted into the superfluid.

can be achieved with an energy mismatch between neighboring fermion sites that exceeds the bandwidth of both the fermions and the phonons. This makes it possible to study the influence of the phonon density of states on the atomic current over the entire phonon band. In addition, it allows us to observe negative differential conductance [11,13,19], which is realized in a solid-state system with difficulty by resorting to semiconductor superlattices [15,18,23]. Last, the parameters of our system can be chosen to ensure that Landau-Zener tunneling to higher fermion bands—often a significant effect in high field transport [18]—is negligible despite the large lattice tilts [13] justifying the use of a tight-binding framework.

The key experimental techniques required for our scheme are twofold: first, the independent trapping of atoms of different species in species-specific optical lattice potentials [24,25] and, second, the tunability of the boson-boson and boson-fermion interactions by Feshbach resonances [5,26]. Also, we exploit the possibility of implementing low-dimensional systems by strongly increasing the depth of the optical potentials along specific directions. In this way effectively one-dimensional systems can be realized by tightly confining atoms to an array of tubes [2].

The structure of this article is as follows: In Sec. II we start from the Bose-Fermi Hubbard model and outline the effective description of the Bose-Fermi mixture in terms of Bogoliubov phonons and Wannier-Stark states. In Sec. III we derive a general expression for the drift velocity of the fermions and show that this expression encompasses the phenomena of negative differential conductance and phonon resonances. Section IV contains the results of a near-exact numerical simulation of a realistic experimental procedure to determine the dependence of the atomic current on the lattice tilt. We end with the conclusions in Sec. V.

## II. EFFECTIVE MODEL

The specific system we consider consists of a homogeneous, one-dimensional Bose-Fermi mixture of bosons and spin-polarized fermions, both trapped in *separate* optical lattice potentials. If the potentials are sufficiently deep so that only the lowest Bloch band is occupied, then the Bose-Fermi mixture can be described by the Bose-Fermi Hubbard model [27]

$$\hat{H}_{bf} = -J_b \sum_{\langle i,j \rangle} \hat{a}_i^\dagger \hat{a}_j - J_f \sum_{\langle i,j \rangle} \hat{c}_i^\dagger \hat{c}_j + \sum_j (j\Delta) \hat{c}_j^\dagger \hat{c}_j + \frac{1}{2} U_b \sum_j \hat{a}_j^\dagger \hat{a}_j^\dagger \hat{a}_j \hat{a}_j + U_{bf} \sum_j \hat{a}_j^\dagger \hat{a}_j \hat{c}_j^\dagger \hat{c}_j, \quad (1)$$

where  $\langle i,j \rangle$  denotes the sum over nearest neighbors. The operators  $\hat{a}_j^\dagger$  ( $\hat{a}_j$ ) create (annihilate) a boson and, similarly, the operators  $\hat{c}_j^\dagger$  ( $\hat{c}_j$ ) create (annihilate) a spinless fermion in a Wannier state localized at site  $j$ . The bosonic and fermionic hopping parameters are  $J_b$  and  $J_f$ , respectively, and the on-site boson-boson and boson-fermion interactions are characterized by the energies  $U_b$  and  $U_{bf}$ , both positive and independently tunable. In contrast to the bosons, the lattice potential of the fermions is assumed to be tilted with an energy splitting  $\Delta \geq 0$  between adjacent sites.

At low temperatures and for sufficiently small boson-boson interactions  $U_b/J_b \sim 1$  most bosons are in the superfluid

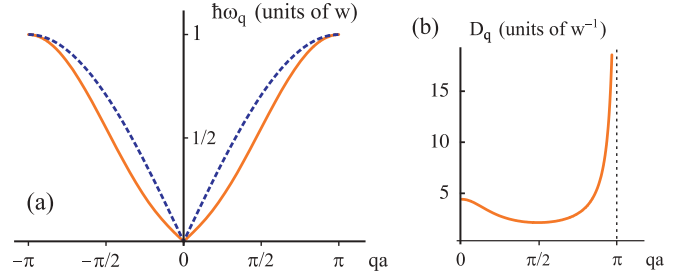


FIG. 2. (Color online) The dispersion relation of acoustic phonons in a solid with  $\hbar\omega_q \sim |\sin(qa/2)|$  (dashed line) and of Bogoliubov phonons in a superfluid confined to an optical lattice (full line) in units of the bandwidth  $w = 4J_b\sqrt{1 + U_b n_b/2J_b}$  for the parameters  $U_b n_b/J_b = 0.5$ . (b) The corresponding density of states  $D_q = |\partial\hbar\omega_q/\partial(qa)|^{-1}$  (full line) of the Bogoliubov phonons is approximately constant for small momenta and exhibits a Van Hove singularity near the edge of the first Brillouin zone (dashed line).

phase and accurately described by the phononic excitations of the superfluid. This description is obtained by transferring the bosonic part of the Hamiltonian  $\hat{H}_{bf}$  into momentum space and adopting the Bogoliubov approach [28], which results in the phonon Hamiltonian

$$\hat{H}_{ph} = \sum_q \hbar\omega_q \hat{b}_q^\dagger \hat{b}_q. \quad (2)$$

Here,  $q$  is the momentum running over the first Brillouin zone, i.e.,  $-\pi/a < q \leq \pi/a$  with  $a$  the lattice spacing, and the bosonic operators  $\hat{b}_q^\dagger$  ( $\hat{b}_q$ ) create (annihilate) a Bogoliubov phonon. The excitation spectrum of the phonons is given by the Bogoliubov dispersion relation  $\hbar\omega_q = \sqrt{E_q(E_q + 2U_b n_b)}$ , where  $n_b$  is the bosonic occupation number and  $E_q = 4J_b \sin^2(qa/2)$  is the dispersion relation of noninteracting bosons in the optical lattice. The dispersion of the Bogoliubov phonons, albeit not identical, is remarkably similar to the dispersion of acoustic phonons in a solid-state system with  $\hbar\omega_q \sim |\sin(qa/2)|$ , shown in Fig. 2(a). The common features are a linear dispersion in the limit  $q \rightarrow 0$  and the band structure with a gap at the boundary of the first Brillouin zone. It should be pointed out that the accuracy of the Bogoliubov description of phonons has been demonstrated experimentally [22], thus we have perfect knowledge of and control over the phonons in our system.

The fermions confined to the tilted potential are represented by the eigenstates of the fermionic part of  $\hat{H}_{bf}$ , i.e., the Wannier-Stark states [29,30]. The unitary transformation that relates the Wannier operators  $\hat{c}_j$  to the Wannier-Stark operators  $\hat{d}_j$  is given by

$$\hat{d}_j = \sum_i \mathcal{J}_{i-j}(2J_f/\Delta) \hat{c}_i, \quad (3)$$

where  $\mathcal{J}_n(z)$  are Bessel functions of the first kind [31]. It follows immediately from the properties of the Bessel functions  $\mathcal{J}_n(z)$  that the Wannier-Stark states are centered at lattice site  $j$  and have a width of the order of  $J_f/\Delta$ . By invoking the identities for the Bessel functions  $\sum_n \mathcal{J}_{n-m}(z) \mathcal{J}_{n-m'}(z) =$

$\delta_{m,m'}$  and  $(2n/z)\mathcal{J}_n(z) = \mathcal{J}_{n+1}(z) + \mathcal{J}_{n-1}(z)$  one finds that the transformed fermionic part of  $\hat{H}_{bf}$  takes the diagonal form

$$\hat{H}_{ws} = \sum_j (j\Delta)\hat{d}_j^\dagger\hat{d}_j. \quad (4)$$

The spectrum of  $\hat{H}_{ws}$  constitutes a so-called Wannier-Stark ladder [29,30] with a constant energy separation  $\Delta$  between adjacent sites, shown in Fig. 1. We emphasize that the Wannier-Stark states are stationary and hence a net current of fermions along the tilted lattice only develops in presence of additional relaxation processes. In particular, it results from the inverse of the transformation in Eq. (3) that a fermion initially localized at a single lattice site undergoes coherent Bloch oscillations with frequency  $\Delta/\hbar$  [7].

To rewrite the boson-fermion interaction in terms of Bogoliubov phonons and Wannier-Stark states we apply the same transformations as for the purely bosonic and fermionic parts of  $\hat{H}_{bf}$ . Invoking the results established in Refs. [28,29] we find the fermion-phonon interaction Hamiltonian

$$\hat{H}_{int} = U_{bf}n_b \sum_j \hat{d}_j^\dagger\hat{d}_j + \sum_{j,\ell,q} [f_{q,\ell}\hat{b}_q e^{-iqaj} + \text{H.c.}] \hat{d}_{j+\ell}^\dagger\hat{d}_j \quad (5)$$

with the corresponding matrix elements

$$f_{q,\ell} = U_{bf} \left( \frac{n_b E_q}{N\hbar\omega_q} \right)^{1/2} \mathcal{J}_\ell \left( \frac{4J_f}{\Delta} \sin \frac{qa}{2} \right) i^\ell e^{-iqa\ell/2}, \quad (6)$$

where  $N$  is the number of lattice sites. We note that  $\hat{H}_{int}$  coincides exactly with the description of the electron-phonon interactions in a solid-state system [29] and thus is perfectly adequate for investigating related phonon effects.

The fermion-phonon interaction  $\hat{H}_{int}$  describes the creation of a Bogoliubov phonon out of the superfluid phase and the reverse process, both caused by the hopping process of the fermions. These incoherent processes involving a single phonon enable fermions to make transitions between Wannier-Stark states separated by  $\ell$  lattice sites. On the other hand, coherent processes resulting from  $\hat{H}_{int}$ , in which a virtual phonon is emitted and reabsorbed, lead to a phonon-mediated fermion-fermion interaction, a renormalized fermion hopping, and a mean-field energy shift of the fermions [12,13].

The effective fermion-fermion interaction, being short range, can be safely neglected if we assume a filling factor of the fermions much lower than 1. However, we have to take into account the renormalization of the fermion hopping  $J_f$  when comparing our theoretical model to experimental or numerical results. As expected from theoretical considerations [12,13] and confirmed by the numerical results in Sec. IV, the renormalization reduces the bare hopping. Last, the mean-field energy shift is explicitly given by  $U_{bf}n_b + \sum_q |f_{q,0}|^2/\hbar\omega_q$ , which is readily determined in the regime  $U_b n_b/J_b \ll 1$  by taking the continuum limit.<sup>1</sup> For a single delocalized fermion with  $J_f/\Delta \gg 1$  the shift is simply  $U_{bf}n_b$ , whereas for a localized

fermion with  $J_f/\Delta \ll 1$  we find  $U_{bf}n_b(1 - aU_{bf}/2\hbar c_s)$ , with  $c_s = (a/\hbar)\sqrt{2J_b U_b n_b}$  the speed of sound in the superfluid.

It is essential for our model that neither interactions with the fermions nor the trapping potential confining the fermions destroy the phononic excitations of the superfluid. These conditions are met by using species-specific optical lattice potentials [24,25] and by limiting the number of fermions in the system [3–5]. Moreover, we restrict our analysis to fermions moving slower than superfluid critical velocity, which is  $c_s$  according to Landau's criterion [32], to avoid excitations other than those caused by the hopping transitions. More precisely, we consider the parameter regime  $\zeta = 2aJ_f/\hbar c_s \ll 1$ , where  $2aJ_f/\hbar$  is the maximal group velocity of the fermions in the lowest Bloch band.

### III. ATOMIC CURRENTS

Since the number of fermions is significantly smaller than number of bosons we effectively treat the superfluid as a phonon bath. Accordingly we describe the dynamics of the fermions by a master equation for the probabilities  $P_j$  that a fermion occupies a Wannier-Stark state at site  $j$ . The master equation reads

$$\partial_t P_i = \sum_j [P_j(1 - P_i)W_{j \rightarrow i} - P_i(1 - P_j)W_{i \rightarrow j}], \quad (7)$$

where  $W_{i \rightarrow j}$  are the rates for a phonon-assisted transition from site  $i$  to site  $j$  and the factors  $(1 - P_j)$  take the Pauli exclusion principle into account. The probabilities  $P_i$  either describe the occupation of a single fermion or the distribution of an ensemble of fermions; in both cases we choose  $\sum_j P_j = 1$ . The average position  $\bar{x}$  of the fermions at time  $t$  is accordingly  $\bar{x} = \sum_j (aj)P_j$  and the average drift velocity  $\bar{v}_d$ , which quantifies the atomic current along the lattice, is given by  $\bar{v}_d = \partial_t \bar{x} = \sum_j (aj)\partial_t P_j$ .

To obtain a useful expression for the drift velocity  $\bar{v}_d$  we exploit the fact that the system is homogeneous so that the transition rates  $W_{i \rightarrow j}$  only depend on the jump distance  $\ell = i - j$ , where jumps with  $\ell > 0$  are defined to be downward the tilted lattice, as depicted in Fig. 1. By using Fermi's golden rule based on the interaction Hamiltonian  $\hat{H}_{int}$ , i.e., to second order in the coupling  $U_{bf}$ , we find

$$W_\ell^E = \frac{2\pi}{\hbar} \sum_q |f_{q,\ell}|^2 (N_q + 1) \delta(\hbar\omega_q - \ell\Delta), \quad (8)$$

$$W_\ell^A = \frac{2\pi}{\hbar} \sum_q |f_{q,\ell}|^2 N_q \delta(\hbar\omega_q - \ell\Delta),$$

where  $N_q = (e^{\hbar\omega_q/k_B T} - 1)^{-1}$  is the mean number of phonons with momentum  $q$  in the superfluid at temperature  $T$  and  $k_B$  is Boltzmann's constant. The rate  $W_\ell^E$  ( $W_\ell^A$ ) corresponds to the process, where a fermion jumps  $\ell$  sites down (up) the lattice and thereby emits (absorbs) a single phonon of energy  $\ell\Delta$ . The expressions for the jump rates  $W_\ell^E$  and  $W_\ell^A$  are valid as long as heating effects caused by the emitted phonons are negligible.

<sup>1</sup>Explicitly, the continuum limit of the sum over all momenta in the lowest band is  $(Na)^{-1} \sum_q \rightarrow \int_{-\pi/a}^{\pi/a} dq/2\pi$ .

To determine  $\bar{v}_d$  in terms of transition rates we substitute the expression in Eq. (7) for  $\partial_t P_j$  and find after some rearrangement that

$$\bar{v}_d = \sum_{j, \ell > 0} (a\ell) [W_\ell^0 P_j (1 - P_{j+\ell}) - W_\ell^A P_j (P_{j+\ell} - P_{j-\ell})] \quad (9)$$

with  $W_\ell^0 = (2\pi/\hbar) \sum_q |f_{q,\ell}|^2 \delta(\hbar\omega_q - \ell\Delta)$  the phonon emission rate at zero temperature. The first term in the sum in Eq. (9) vanishes if the fermions are degenerate at zero temperature with all lattice sites  $j \geq j_c$  occupied, i.e.,  $P_j = 1$  for  $j \geq j_c$  and  $P_j = 0$  for  $j < j_c$  with  $j_c$  fixed by the number of fermions, whereas the second term represents finite temperature effects. For the system far from degeneracy and for small fermion occupation numbers we may make the approximation  $P_i P_j \approx 0$  and use the condition  $\sum_j P_j = 1$ , which yields  $\bar{v}_d = \sum_{\ell > 0} (a\ell) W_\ell^0$  for the drift velocity. We note that at this level of approximation the expression for the drift velocity and all subsequent analytical considerations apply, *mutatis mutandis*, also to lattice Bose-Bose mixtures [21].

Taking the continuum limit of the sum over all phonon momenta (appearing in  $W_\ell^0$ ) and integrating over the first Brillouin zone we finally obtain

$$\bar{v}_d = \frac{a^2 N}{\hbar} \sum_{\ell > 0}^{\ell_{\max}} \ell \left| \frac{\partial \hbar\omega_q}{\partial q} \right|^{-1} |f_{q,\ell}|^2 |_{q=q_\ell}, \quad (10)$$

with  $q_\ell$  implicitly defined by  $E_{q_\ell} = \sqrt{(\ell\Delta)^2 + (U_b n_b)^2} - U_b n_b$ . The latter relation also yields the maximum jump distance  $\ell_{\max}$ , which is compatible with energy conservation in the fermion-phonon relaxation process. We see from Eq. (10) that the total drift velocity  $\bar{v}_d$  is determined by the sum over all admissible jump distances  $\ell$  weighted by the phonon density of states  $|\partial \hbar\omega_q / \partial q|^{-1}$  and the fermion-phonon coupling  $|f_{q,\ell}|^2$ .

We first determine the mobility  $\mu$  of the fermions in the Ohmic regime, which we define by the relation  $\bar{v}_d = \mu\delta$  in the limit  $\delta \rightarrow 0$ , where  $\delta = \Delta/4J_b$  is approximately the ratio of the lattice tilt and the phonon bandwidth for the small values of  $U_b n_b / J_b$  we consider here. We find that  $\bar{v}_d / \delta \propto \sum_{\ell=1}^{\infty} \ell^2 \mathcal{J}_\ell^2(\ell\zeta)$  for  $\delta \rightarrow 0$ , with  $\zeta = 2aJ_f / \hbar c_s$  as previously defined. This sum is a Kapteyn series of the second kind, for which a closed form is known [31], yielding for the mobility

$$\mu = \frac{aU_{bf}^2}{8\sqrt{2}U_b\hbar} \left( \frac{J_b}{U_b n_b} \right)^{1/2} \frac{\zeta^2(\zeta^2 + 4)}{(1 - \zeta^2)^{7/2}}. \quad (11)$$

The mobility diverges in the limit  $\zeta \rightarrow 1$ , however, it is well defined in the regime  $\zeta \ll 1$ . For the practically important case, where the potential depth for the fermions and hence the hopping parameter  $J_f$  is varied, the mobility scales as  $\mu \sim J_f^2$  in the limit  $J_f \rightarrow 0$ .

The dependence of the drift velocity  $\bar{v}_d$  given in Eq. (10) on the full range of accessible lattice tilts  $\delta$  is shown in Fig. 3. We see that the atomic current makes a sharp transition from Ohmic conductance to negative differential conductance. The main reason is that the width of the Wannier-Stark states, proportional to  $J_f / \Delta$ , and hence the overlap between states at different sites decreases as the tilt  $\Delta$  is increased. This reduced overlap results in a low drift velocity  $\bar{v}_d$ —in analogy to NDC

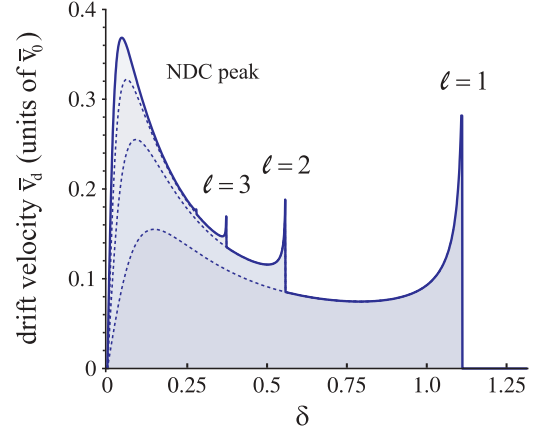


FIG. 3. (Color online) The total drift velocity  $\bar{v}_d$  (full line) as a function of the lattice tilt  $\delta = \Delta/4J_b$ . The contributions from different jump distances  $\ell$  (dashed lines) result in a distinct NDC peak and a series of phonon resonances at the positions  $\delta \approx 1/\ell$ . The system parameters are  $U_b n_b / J_b = 0.5$ ,  $J_f / J_b = 0.4$  yielding for the phonon bandwidth  $1.12 \times 4J_b$  and  $\zeta = 0.5$ . The drift velocity is given in units of  $\bar{v}_0 = a n_b U_{bf}^2 / 4J_b \hbar$ .

in semiconductor superlattices [15,18]—and is determined by the matrix elements  $f_{q,\ell}$ . The drift velocity  $\bar{v}_d$  depends on the tilt as  $(J_f / \Delta)^{2\ell}$  for each jump distance  $\ell$  in the limit of small fermionic bandwidth  $J_f / \Delta \ll 1$ , which can be readily achieved in cold atom systems. As can be seen in Fig. 3 the NDC is particularly pronounced due to the superposed contributions from different jump distances  $\ell$  to the total current. These findings are in accordance with predictions for a free homogeneous superfluid [11,13,19]; however, the result for  $\bar{v}_d$  in Eq. (10) describes additional features stemming from the influence of the phonon density of states.

Specifically, the drift velocity exhibits anomalies in the form of sharp peaks, which correspond to the anticipated electron-phonon resonances in a solid-state system [14,16]. As shown in Fig. 2(b), the phonon density of states  $|\partial \hbar\omega_q / \partial q|^{-1}$  is approximately constant for small momenta, but exhibits a Van Hove singularity [20] at the edge of the first Brillouin zone. Therefore phonon resonances arise as the momentum of the emitted phonons approaches the edge of the phonon band. It can be found from Eq. (10) that the resonance condition is given by  $\ell\delta = \sqrt{1 + U_b n_b / 2J_b}$  with  $\ell = 1, 2, \dots, \ell_{\max}$  and thus the current displays a peak at  $\delta \approx 1/\ell$  corresponding to each admissible jump distance  $\ell$ . Since the fermion-phonon interaction provides the only relaxation process in the system these anomalies are directly reflected in the tilt dependence of the current. Further, the current vanishes as the lattice tilt exceeds the phonon bandwidth because there are no phonon states available in order to dissipate energy into the superfluid.

Let us briefly discuss the effect of an additional (shallow) harmonic trapping potential of the bosons on the phonon resonances. If the system is aligned along the  $x$  axis the potential takes the form  $V(x) = m_b \omega_x^2 x^2 / 2$  with the trap frequency  $\omega_x$ . In the experimentally relevant case, where the harmonic oscillator length  $l_x = \sqrt{\hbar / m_b \omega_x}$  satisfies the condition  $l_x / N \gg n_b a$ , the local density approximation (LDA) is applicable [27,33]. The LDA consists of replacing the bosonic density  $n_b$  by the position-dependent density  $n_b(x)$ ,

determined by  $V(x)$ , with the other parameters of the model unmodified. Consequently, the average drift velocity in Eq. (10) has to be replaced by  $\bar{v}_d^{\text{LDA}} = \int dx p(x) \bar{v}_d[n_b(x)]$ , where  $p(x)$  denotes the normalized spatial distribution of the fermions. This averaging might cause some broadening of the phonon resonances. However, the position of the resonances  $\delta = \ell^{-1} \sqrt{1 + U_b n_b / 2J_b}$  and more generally  $\bar{v}_d$  (except for the prefactor  $\bar{v}_0$ ) depend on  $n_b$  only through the expression  $U_b n_b / J_b \ll 1$ . Thus the trap-induced broadening can be made arbitrarily small by reducing the boson-boson interaction energy  $U_b$ , which sets the smallest energy scale close to resonance. This is partly explained by the fact that the resonances involve only phonons from the upper edge of the phonon band with wavelengths comparable to the lattice spacing  $a$ .

#### IV. NUMERICAL SIMULATION

The theoretical results derived in the previous section are, strictly speaking, valid for stationary atomic currents in a homogeneous system. We now show based on numerical simulations that the predicted negative differential conductance and the phonon resonances are observable in a system of finite size under the conditions of a realistic measuring procedure. In order to measure the atomic current in an experimental setup we envisage a procedure consisting of the following three steps:

(a) Initially, both the bosons and fermions are prepared in a horizontal optical lattice and the total system is in equilibrium.<sup>2</sup> The fermions are each localized in separate sites sparsely distributed through the fermionic lattice of sufficient depth so that  $P_i P_j \approx 0$  holds. In this configuration the fermions are automatically cooled by the surrounding superfluid [34], which is only slightly distorted [13].

(b) Subsequently, the lattice of the fermions is tilted for a fixed evolution time  $\tau$  of the order of  $\hbar/J_f$  to let them evolve. To obtain a detectable displacement of the fermions the fermionic hopping  $J_f$  may have to be increased by reducing the depth of the lattice.

(c) Finally, the spatial distribution of the fermions is detected, e.g., by *in situ* single-atom resolved imaging [35,36]. From the difference between the initial and final distributions it should be possible to extract a reliable estimate for the atomic current. Alternatively, the momentum distribution and hence the drift velocity of the fermions may be determined directly by a time-of-flight measurement.

To demonstrate the feasibility of this procedure we have simulated the fully coherent dynamics at zero temperature of both the bosons and fermions based on the complete Bose-Fermi Hubbard model given in Eq. (1). To this end we have used the time-evolving block decimation (TEBD) algorithm [37], which is essentially an extension to the well-established density matrix renormalization group (DMRG) method [38,39]. The TEBD algorithm permits the near-exact dynamical simulation of quantum many-body systems

<sup>2</sup>Our numerical simulations show that the total equilibration of the system is not an essential requirement for the procedure to work. We obtain similar results if the fermions are immersed into the superfluid in a nonadiabatic way.

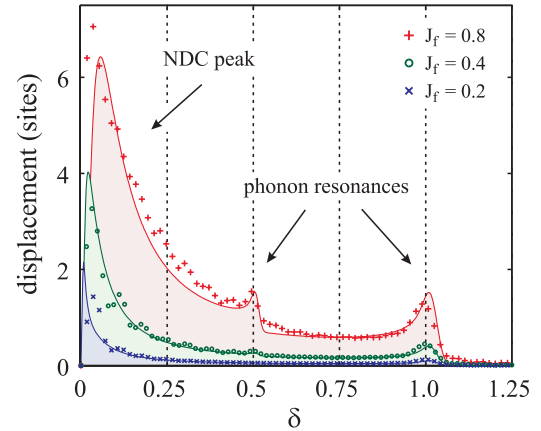


FIG. 4. (Color online) The displacement of the fermion as a function of the lattice tilt  $\delta$  determined numerically (symbols  $+$ ,  $\circ$ ,  $\times$ ) and corresponding analytical fits (solid lines). The dominant NDC peak and the  $\ell = 1$  phonon resonance at the boundary of the phonon band can be clearly recognized. The ratio  $V$  between the height of the  $\ell = 1$  resonance and the NDC peak is  $V = \{0.09, 0.14, 0.18\}$  for increasing  $J_f$ . The  $\ell = 2$  resonance is visible for sufficiently large fermionic hopping  $J_f$ . The system parameters are  $J_f = \{0.2, 0.4, 0.8\}$ ,  $U_b = 0.1$ ,  $U_{bf} = 0.5$  and the fitting parameters are  $\varepsilon = 0.1$ ,  $\bar{J}_f = 0.7J_f$ ,  $\ell_{\text{max}} = 2$ , with energies in units of  $J_b$ .

far from equilibrium, which is crucial for our purposes. The experimental procedure was simulated for a system consisting of 101 lattice sites with a bosonic filling factor  $n_b = 1$  and a single fermion initially located at the center of the lattice. We used box boundary conditions and the evolution time was limited to  $\tau = 24\hbar/J_b$  to minimize finite-size effects, primarily reflections of phonons from the boundaries.

Figure 4 shows the displacement of the fermion as a function of the lattice tilt  $\delta$  for a set of realistic experimental parameters, in particular, for three different values of the fermion hopping  $J_f$ . The main features predicted by our theoretical analysis can be clearly recognized, namely the dominant NDC peak, the phonon resonance at  $\delta \approx 1$  corresponding to the jump distance  $\ell = 1$ , and the suppression of the current for  $\delta \gg 1$ . In addition, for sufficiently large values of  $J_f$  the phonon resonance at  $\delta \approx 1/2$  corresponding to the jump distance  $\ell = 2$  is visible. For lower values of  $J_f$  the phonon resonance for  $\ell = 2$  may still lead to a characteristic drop in the current once the lattice tilt exceeds half the phonon bandwidth. The resonances for higher values of the jump distance  $\ell$  seem to be masked mainly by broadening effects for the parameter regimes tested.

The ratio between the height of the  $\ell = 1$  phonon resonance and the NDC peak, i.e., their relative visibility  $V$ , depends nontrivially on the fermion hopping  $J_f$ . The hopping  $J_f$  enters the expression for  $\bar{v}_d$  in Eq. (10) through the matrix elements  $f_{q,\ell}$  in the form of  $\mathcal{J}_\ell(s\ell J_f/J_b)$ , where the parameter  $s$  depends on the lattice tilt. Close to resonance we have  $s \approx 1$ , whereas for small tilts  $\ell\Delta \ll U_b n_b$  we obtain  $s \approx \sqrt{2J_b/U_b n_b}$  and hence  $s \gg 1$  in the superfluid regime. Accordingly, the height of the  $\ell = 1$  phonon resonance ( $s \approx 1$ ) varies only slowly with  $J_f$  as opposed to the height of the NDC peak ( $s \gg 1$ ), which is characterized by the oscillatory nature of the Bessel functions.

Thus a careful choice of  $J_f$  allows us to optimize the visibility  $V$ , i.e., to minimize the height of the NDC peak, by tuning  $s\ell J_f/J_b$  close to a zero of the relevant Bessel functions. For the increasing values of  $J_f$  considered in our simulation the first zero of the Bessel function  $\mathcal{J}_2(z)$  is approached, which explains the improved visibility  $V$  for higher  $J_f$ , shown in Fig. 4.

The general broadening of the phonon resonances may be caused by finite-size effects and multiphonon processes. The finite-size effects include reflections of phonons from the boundary of the system that in turn affect the motion of the fermion. Multiphonon processes, which have been neglected in our theoretical analysis, also cause some broadening of the single-phonon resonances. In particular the continuous drop in the current to zero can be explained by the emission of several low-energy phonons during a jump process, which is allowed even if the lattice tilt exceeds the phonon bandwidth.

In order to compare the numerical and the theoretical results, at least qualitatively, we adapt our expression for the drift velocity  $\bar{v}_d$  to a system of finite size. In addition, we introduce the observed broadening effects characterized by the energy  $\varepsilon$  into the theory. Explicitly, we calculate the average drift velocity by using the expression  $\bar{v}_d^\varepsilon = \sum_{\ell>0}^{\ell_{\max}} (a\ell) W_\ell^\varepsilon$  with the rates  $W_\ell^\varepsilon = (2\pi/\sqrt{\pi\varepsilon\hbar}) \sum_q |f_{q,\ell}|^2 \exp[-(\hbar\omega_q - \ell\Delta)^2/\varepsilon^2]$ . The rates reduce to the previous expression  $W_\ell^0$  in absence of broadening, i.e.,  $\lim_{\varepsilon\rightarrow 0} W_\ell^\varepsilon = W_\ell^0$ . The average displacement of the fermion (in units of lattice sites) after the evolution time  $\tau$  is then approximately given by  $\bar{x}_a \approx \bar{v}_d^\varepsilon \tau/a$ .

We fit this theoretical model to the numerical results with the broadening  $\varepsilon$ , the maximal jump distance  $\ell_{\max}$ , and the *effective* fermionic hopping  $\tilde{J}_f$  as free parameters. The first two parameters allow us to extract a quantitative value for the broadening and to determine the dominant hopping process in the experiment. The fermionic hopping needs adjustment because the bare hopping  $J_f$  is renormalized by coherent phonon processes, which lead to a reduced hopping  $\tilde{J}_f < J_f$  as discussed in Refs. [12,13]. This is in direct analogy to the increased effective mass of polarons due to the drag of the phonon cloud [40].

As can be seen in Fig. 4 the fit describes the numerical results very accurately with moderate broadening  $\varepsilon$  and a minor reduction of the fermionic hopping  $J_f$ . Further, we find that  $\ell_{\max} = 2$  and thus the dominant transport processes are nearest- and next-nearest-neighbor hopping; this is consistent with the absence of higher-order phonon resonances noted earlier. The high level of agreement between our theoretical model and the numerical results is partly explained by two observations: First, the numerical results show that the fermion reaches a constant drift velocity on a time scale much shorter than the evolution time  $\tau$ , thus transient effects due to the sudden tilting of the lattice are negligible. Second, the drift velocity remains approximately constant over the entire evolution time, as illustrated in Fig. 5, resulting in a stationary atomic current.

Since our numerics simulates the full dynamics of the system we can monitor the average position of the fermion at different evolution times  $\tau$  and extend the range of parameters considered so far. In particular, we are interested in the atomic current in presence of strong boson-fermion

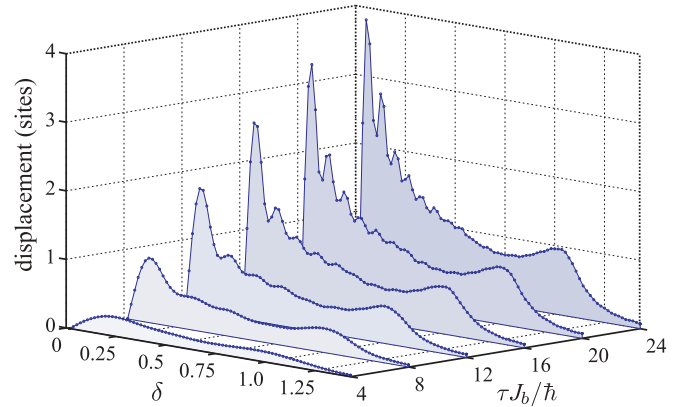


FIG. 5. (Color online) The displacement of the fermion as a function of the lattice tilt  $\delta$  for different evolution times  $\tau$  determined numerically (connected data points). The NDC peak and the  $\ell = 1$  phonon resonance are clearly visible also in presence of strong boson-fermion and boson-boson interactions. The additional peaks between the NDC peak and the phonon resonance are due to finite-time effects. The displacement increases approximately linearly with the evolution time  $\tau$ . The system parameters are  $J_f = 0.5$ ,  $U_b = U_{bf} = 1$ , with energies in units of  $J_b$ .

and boson-boson interactions, where our theory, assuming a superfluid phase, is no longer applicable. Figure 5 shows the displacement of the fermion as a function of the lattice tilt  $\delta$  for the interaction strengths  $U_b = U_{bf} = J_b$  and for different evolution times  $\tau$ . We see that the NDC peak and the  $\ell = 1$  phonon resonance are not noticeably affected by the presence of strong interactions, thus they both seem to be robust features of the atomic current. We note that the additional peaks in the displacement-tilt dependence (located between the NDC peak and the  $\ell = 1$  phonon resonance) are due to finite-time effects, which is revealed by a more detailed analysis of the time dependence of the numerical results. Furthermore, we observe an approximately linear increase of the displacement of the fermion with the evolution time—a finding also confirmed for weaker interactions.

## V. CONCLUSIONS

In our analytical and numerical investigation of phonon-assisted atomic currents along a tilted potential we have shown that Bose-Fermi mixtures in optical lattices lend themselves naturally to investigate nonequilibrium transport phenomena present in solid state systems. In more detail, we have formulated an effective model for the Bose-Fermi mixture describing the bosons and fermions in terms of Bogoliubov phonons and Wannier-Stark states, respectively, with a generic fermion-phonon interaction of an identical type to the one encountered in solids.

We have studied the dependence of the atomic current on the lattice tilt from first principles and found that our model accommodates negative differential conductance and phonon resonances. To demonstrate that these features are observable by using ultracold atoms in the context of a finite-size system and a realistic measuring procedure we have calculated the atomic current numerically by using the TEBD algorithm including the full dynamics of both the bosons

and the fermions. Our numerical results show that the phonon resonance at the boundary of the phonon band is a robust phenomenon that occurs over a wide range of system parameters despite broadening, which might be increased by finite temperature effects [13,19] not directly taken into account in our model. Finally, we note that in an obvious extension of this work we will investigate the effect of the transition of the bosons from the superfluid to the Mott insulator regime on the atomic current through the system.

## ACKNOWLEDGMENTS

M.B. thanks the Swiss National Science Foundation for the support through Project No. PBSKP2/130366. M.B., W.B., and A.P. acknowledge financial support from the German Research Foundation (DFG) through SFB 767. S.R.C. and D.J. thank the National Research Foundation and the Ministry of Education of Singapore for support. D.J. acknowledges support from the ESF program EuroQUAM (EPSRC Grant No. EP/E041612/1).

- 
- [1] M. Lewenstein, A. Sanpera, V. Ahufinger, B. Damski, A. Sen, and U. Sen, *Adv. Phys.* **56**, 243 (2007).
- [2] I. Bloch, J. Dalibard, and W. Zwerger, *Rev. Mod. Phys.* **80**, 885 (2008).
- [3] K. Günter, T. Stöferle, H. Moritz, M. Köhl, and T. Esslinger, *Phys. Rev. Lett.* **96**, 180402 (2006).
- [4] S. Ospelkaus, C. Ospelkaus, O. Wille, M. Succo, P. Ernst, K. Sengstock, and K. Bongs, *Phys. Rev. Lett.* **96**, 180403 (2006).
- [5] T. Best, S. Will, U. Schneider, L. Hackermüller, D. van Oosten, I. Bloch, and D.-S. Lühmann, *Phys. Rev. Lett.* **102**, 030408 (2009).
- [6] A. Zenesini, C. Sias, H. Lignier, Y. Singh, D. Ciampini, O. Morsch, R. Mannella, E. Arimondo, A. Tomadin, and S. Wimberger, *New J. Phys.* **10**, 053038 (2008).
- [7] M. Ben Dahan, E. Peik, J. Reichel, Y. Castin, and C. Salomon, *Phys. Rev. Lett.* **76**, 4508 (1996).
- [8] G. Roati, E. de Mirandes, F. Ferlaino, H. Ott, G. Modugno, and M. Inguscio, *Phys. Rev. Lett.* **92**, 230402 (2004).
- [9] C. Sias, H. Lignier, Y. P. Singh, A. Zenesini, D. Ciampini, O. Morsch, and E. Arimondo, *Phys. Rev. Lett.* **100**, 040404 (2008).
- [10] H. Ott, E. de Mirandes, F. Ferlaino, G. Roati, G. Modugno, and M. Inguscio, *Phys. Rev. Lett.* **92**, 160601 (2004).
- [11] A. V. Ponomarev, J. Madroñero, A. R. Kolovsky, and A. Buchleitner, *Phys. Rev. Lett.* **96**, 050404 (2006).
- [12] M. Bruderer, A. Klein, S. R. Clark, and D. Jaksch, *Phys. Rev. A* **76**, 011605(R) (2007).
- [13] M. Bruderer, A. Klein, S. R. Clark, and D. Jaksch, *New J. Phys.* **10**, 033015 (2008).
- [14] V. V. Bryksin and Y. A. Firsov, *Solid State Commun.* **10**, 471 (1972).
- [15] G. H. Döhler, R. Tsu, and L. Esaki, *Solid State Commun.* **17**, 317 (1975).
- [16] V. V. Bryksin and P. Kleinert, *J. Phys. Condens. Matter* **9**, 7403 (1997).
- [17] S. Feng, C. H. Grein, and M. E. Flatté, *Phys. Rev. B* **68**, 085307 (2003).
- [18] K. Leo, *High-Field Transport in Semiconductor Superlattices* (Springer, Berlin, 2003).
- [19] A. R. Kolovsky, *Phys. Rev. A* **77**, 063604 (2008).
- [20] L. Van Hove, *Phys. Rev.* **89**, 1189 (1953).
- [21] J. Catani, L. De Sarlo, G. Barontini, F. Minardi, and M. Inguscio, *Phys. Rev. A* **77**, 011603 (2008).
- [22] P. T. Ernst, S. Götze, J. S. Krauser, K. Pyka, D.-S. Lühmann, D. Pfannkuche, and K. Sengstock, *Nat. Phys.* **6**, 56 (2009).
- [23] L. Esaki and R. Tsu, *IBM J. Res. Dev.* **14**, 61 (1970).
- [24] O. Mandel, M. Greiner, A. Widera, T. Rom, T. W. Hänsch, and I. Bloch, *Phys. Rev. Lett.* **91**, 010407 (2003).
- [25] G. Lamporesi, J. Catani, G. Barontini, Y. Nishida, M. Inguscio, and F. Minardi, *Phys. Rev. Lett.* **104**, 153202 (2010).
- [26] G. Roati, M. Zaccanti, C. D'Errico, J. Catani, M. Modugno, A. Simoni, M. Inguscio, and G. Modugno, *Phys. Rev. Lett.* **99**, 010403 (2007).
- [27] A. Albus, F. Illuminati, and J. Eisert, *Phys. Rev. A* **68**, 023606 (2003).
- [28] D. van Oosten, P. van der Straten, and H. T. C. Stoof, *Phys. Rev. A* **63**, 053601 (2001).
- [29] D. Emin and C. F. Hart, *Phys. Rev. B* **36**, 2530 (1987).
- [30] M. Glück, A. R. Kolovsky, and H. J. Korsch, *Phys. Rep.* **366**, 103 (2002).
- [31] G. N. Watson, *A Treatise on the Theory of Bessel Functions*, 2nd ed. (Cambridge University Press, Cambridge, England, 1995).
- [32] L. D. Landau, *J. Phys. (Moscow)* **5**, 71 (1941).
- [33] M. Krämer, C. Menotti, L. Pitaevskii, and S. Stringari, *Eur. Phys. J. D* **27**, 247 (2003).
- [34] A. J. Daley, P. O. Fedichev, and P. Zoller, *Phys. Rev. A* **69**, 022306 (2004).
- [35] W. S. Bakr, J. I. Gillen, A. Peng, S. Fölling, and M. Greiner, *Nature (London)* **462**, 74 (2009).
- [36] J. F. Sherson, C. Weitenberg, M. Endres, M. Cheneau, I. Bloch, and S. Kuhr, *Nature (London)* **467**, 68 (2010).
- [37] G. Vidal, *Phys. Rev. Lett.* **91**, 147902 (2003).
- [38] S. R. White, *Phys. Rev. Lett.* **69**, 2863 (1992).
- [39] U. Schollwöck, *Rev. Mod. Phys.* **77**, 259 (2005).
- [40] G. D. Mahan, *Many-Particle Physics*, 3rd ed. (Kluwer Academic, New York, 2000).